Proceedings of the Korean Nuclear Society Spring Meeting
Pohang, Korea, May 1999

Thermal Stress Analysis for a Circular Piping Subjected to Internally Stratified Flow

Jong Chull Jo, Young Hwan Choi, Yun Il Kim and Won Ky Shin

Korea Institute of Nuclear Safety
19 Kusung-dong, Yusung-ku, Taejon 305-338, Korea

Abstract

This paper presents an effective numerical method for predicting the transient temperature distributions in a horizontal circular pipe subjected to internally stratified flow. The method employs a body-fitted, non-orthogonal grid system to accommodate the pipe wall of circular geometry and the interface of the two fluids at different temperatures, of which the level is variable. The transient behaviors of fluid flow and temperature distribution in the piping are simulated using the finite volume approach. The convection term is approximated by a higher-order bounded scheme named COPLA, which is known as a high-resolution and bounded discretization scheme. The cell-centered, non-staggered grid arrangement is adopted and the resulting checkerboard pressure oscillation is prevented by the application of modified momentum interpolation scheme. The SIMPLE algorithm is employed for the pressure and velocity coupling. As an illustrative problem, the present method has been applied to the stratified flow in the pressurizer surge line of nuclear reactor, and the results have been discussed in detail. In addition, some stress analyses have been performed for the thermally stratified piping using finite element method(FEM) in this study. Non-dimensional hoop stress and radial stress as a function of time have been obtained along the piping wall. The result shows that the hoop stress near the pipe inner surface decreases rapidly and increases again as the time increases. It means the fatigue damage due to thermal stratification is very large near the pipe inner surface.

1. Introduction

The integrity of piping systems connected to reactor coolant system is susceptible to be threatened by the thermal stratification causing unacceptable stresses in the pipe wall. In piping systems where hot and cold fluids flow in, two fluid layers can be formed due to the difference in fluid density (or temperature). Such piping systems susceptible to the thermal stratification include pressurizer surge lines, emergency core cooling lines, residual heat removal lines, pressurizer spray lines, charging lines etc. Especially, the thermal stratification in the pressurizer surge line has been addressed as one of the significant safety and technical issues in most countries holding nuclear power plants since the USNRC issued Bulletins 88-08 and 88-11[1-2] in 1988, requesting licensees to take proper actions for resolution of the issue. To asses the potential for piping damage due to the thermal stratification, it is necessary, first of all, to determine the transient temperature distributions in the wall of the pipe in which thermally stratified flow exists.

Several investigators[3-6] have made efforts to determine the temperature and stress distributions in the pipe wall by means of laboratory testing of a particular geometry or field measurement of temperatures or fully theoretical predictions. There are much difficulties and limitations in applying the first two approaches for operating plants. Only a few literatures addressing the theoretical analyses are available. Smith et al.[3] presented an approximate analytical solution for the steady-state temperature distributions in a pipe wall. Yu et al.[6] obtained temperature and stress distributions for the steady-state heat transfer model of PWR pressurizer surge line. The model was simplified by using the compute code ANSYS[7] based on the assumptions that the inside of the pipe wall is exposed to two distinct ambient fluids of which the temperatures are constant. Jung et al.[8] proposed an unsteady two-dimensional natural convection model for the same problem as that considered by Yu et al.[6]. However the grid system used in the numerical calculations was not satisfactory to simulate the initial condition of the fluid interface.

This paper presents a numerical method for analyzing stratified flows in horizontal circular pipes. The method presented in this paper employs a body-fitted, non-orthogonal grid system to accommodate the pipe wall of circular geometry and the interface of the two fluids at different temperatures, of which the level is variable. The convection term is approximated by a higher-order bounded scheme named COPLA [9], which is known to be a high-resolution and bounded discretization scheme. The cell-centered, non-staggered grid arrangement is adopted and the resulting checkerboard pressure oscillation is prevented by the application of modified momentum interpolation scheme [10]. The SIMPLE algorithm[11] is employed for the pressure and velocity coupling. This study investigates the effects of the level of interface between the two stratified fluids on the determination of the transient temperature distributions in the piping wall.

In addition, some stress analyses have been performed for the thermally stratified piping using finite element method (FEM), based on the transient temperature distributions in the piping wall. Non-dimensional hoop stress and radial stress as a function of time have been obtained along the piping wall.

2. Heat transfer analysis for the thermally stratified piping

Governing equations

Consider a situation that a specified amount of hot fluid flows into a horizontal circular pipe initially filled with cold fluid at the same temperature of the pipe wall, and then occupies the upper position of the pipe suddenly (see Fig. 1). Consequently this leads to formation of two distinct fluid layers in the pipe. For simplicity, it is assumed that axial conduction through the pipe wall is negligible, the fluids are Newtonian with constant properties and the Boussinesq approximation is valid. Thus the governing equation of this thermally stratified flow inside the pipe can be expressed in a generalized coordinate system x^j as,

$$\frac{\partial}{\partial x^1}U_1+\frac{\partial}{\partial x^2}U_2=0 \tag{1}$$

$$\frac{\partial}{\partial t}(J\rho u_1)+\frac{\partial}{\partial x^1}\left[U_1u_1-\frac{\mu}{J}\left\{\frac{\partial u_1}{\partial x^1}D_1^1+\frac{\partial u_1}{\partial x^2}D_2^1+b_1^1w_1^1+b_2^1w_1^2\right\}+Pb_1^1\right]+\frac{\partial}{\partial x^2}\left[U_2u_1-\frac{\mu}{J}\left\{\frac{\partial u_1}{\partial x^1}D_1^2+\frac{\partial u_1}{\partial x^2}D_2^2+b_1^2w_1^1+b_2^2w_1^2\right\}+Pb_1^2\right]$$
$$=\rho g\beta(T-T_{ref})J \tag{2}$$

$$\frac{\partial}{\partial t}(J\rho u_2)+\frac{\partial}{\partial x^1}\left[U_1u_2-\frac{\mu}{J}\left\{\frac{\partial u_2}{\partial x^1}D_1^1+\frac{\partial u_2}{\partial x^2}D_2^1+b_1^1w_2^1+b_2^1w_2^2\right\}+Pb_2^1\right]+\frac{\partial}{\partial x^2}\left[U_2u_2-\frac{\mu}{J}\left\{\frac{\partial u_2}{\partial x^1}D_1^2+\frac{\partial u_2}{\partial x^2}D_2^2+b_1^2w_2^1+b_2^2w_2^2\right\}+Pb_2^2\right]=0 \tag{3}$$

$$\frac{\partial}{\partial t}(J\rho C_pT)+\frac{\partial}{\partial x^1}\left[U_1C_pT-\frac{k}{J}\left\{\frac{\partial T}{\partial x^1}D_1^1+\frac{\partial T}{\partial x^2}D_2^1\right\}\right]+\frac{\partial}{\partial x^2}\left[U_2C_pT-\frac{k}{J}\left\{\frac{\partial T}{\partial x^1}D_1^2+\frac{\partial T}{\partial x^2}D_2^2\right\}\right]=0 \tag{4}$$

where

$$U_1=\rho(u_1b_1^1+u_2b_2^1),\quad U_2=\rho(u_1b_1^2+u_2b_2^2),\quad D_m^j=b_k^jb_k^m,\ \text{and}\quad w_j^i=\frac{\partial u_i}{\partial x^k}b_j^k \tag{5}$$

and the geometric coefficients b_i^j represent the cofactors of $\partial y^i/\partial x^j$ in the Jacobian matrix of the coordinate transformation $y^i=y^i(x^j)$, J stands for the determinant of the Jacobian matrix and y^i is the Cartesian coordinate system. In the above equations (1) - (4), ρ, μ, p, k, c_p, β, and g denote respectively density, viscosity, pressure, thermal conductivity, the specific heat, volumetric coefficient of thermal expansion, and the gravitational acceleration. In addition, T_{ref} and u_i are the reference temperature and the Cartesian velocity components in the y^i direction, respectively.

Initial and boundary conditions

As mentioned previously, the pipe wall is initially at the temperature of cold fluid T_c, and is suddenly exposed to hot fluid at T_h. The initial conditions for this problem are given as

$u_i=0$ ($i=1,2$) in the whole solution domain, $t=0$ (6a)

$T=T_c$ in the pipe wall and the cold fluid layer, $t=0$ (6b)

$T=T_h$ in the hot fluid layer, $t=0$ (6c)

where the subscripts *c* and *h* stand for cold and hot, respectively.

Because the solution domain is symmetrical thermally and geometrically, only half of the region is needed to analyze. Thus along the symmetry line, the symmetry boundary conditions will be applied for both velocity and temperature. On the solid wall, the velocity of fluid vanishes. For this situation the boundary conditions are given by

$u_i=0$ ($i=1,2$) at the inner surface of the pipe, $t>0$ (7a)

$-k\left.\frac{\partial T}{\partial n}\right|_{x^2}=h(T-T_\infty)$ at the outer surface of the pipe, $t>0$ (7b)

$u_2=0$, $\frac{\partial u_1}{\partial x^1}=0$, $\frac{\partial T}{\partial x^1}=0$ at the symmetry plane, $t>0$ (7c)

where *n* is the outward normal to the surface of the wall, T_∞ is the temperature of environment outside the pipe, and *h* is heat transfer coefficient.

Solution domain discretization

The governing equations (1) – (4) are solved numerically by a finite volume approach, requiring the discretization of the solution domain into a finite number of quadrilateral control volume cell whose faces are coincided with the non-orthogonal curvilinear coordinate lines. A typical discretized domain is presented in Fig. 2, and also a typical control volume cell is shown in Fig. 3. The values of all computed variables are stored at the geometric center of each control volume cell. The interface between the hot and cold fluids is arranged here to align with a boundary between two rows of cells, i.e. a gridline.

To obtain the curvilinear non-orthogonal mesh shown in Fig. 2, it is assumed that the solution domain is the cross-section of a pair of eccentric cylinders as shown in Fig. 3. The center of the inner solid cylinder is coincided with the intersecting point of the fluid interface and the vertical symmetry line passing the center of the pipe. The outer cylinder is the pipe subjected to internally stratified flow, and the inner cylinder has such a small size of diameter that the effect of its presence on the calculations can be negligible. Thus, the following boundary conditions are applied to the outer surface of the infinitesimal inner solid cylinder with such an infinitesimal diameter.

$$\frac{\partial u_i}{\partial x^2} = 0 \ , \quad \frac{\partial T}{\partial x^2} = 0 \quad (i = 1, 2) \text{ at the outer surface of the infinitesimal inner cylinder, } \quad t \rangle 0 \tag{8}$$

Dislocating the inner solid cylinder either downward or upward can easily control the level of the fluid interface having a horizontal straight-line configuration. For this situation, it is needed only to analyze half region of the solution domain.

The grid is generated for a half symmetric region of the solution domain by using an algebraic method. The straight lines are the equally spaced radial lines passing through the centerline of the inner cylinder. Then the line segments are divided by some algebraic formula. In this study, the calculations are performed with a grid of 52×42, forming 51 divisions in the circumferential direction and 41 divisions in the radial direction.

Discretization of governing equation

In this study, the discretization of the governing equations is performed following the finite volume approach, and the convection terms are approximated by the COPlA scheme developed by Choi et al.[9] and the unsteady term is treated by the backward differencing scheme[11]. The resulting algebraic equation for a variable $\boldsymbol{j}$ can be written in the following general form.

$$A_P \boldsymbol{j}_P = A_E \boldsymbol{j}_E + A_W \boldsymbol{j}_W + A_N \boldsymbol{j}_N + A_S \boldsymbol{j}_S + b_j \tag{9}$$

where $A_j \, (j = P, E, W, N \text{ or } S)$ are coefficients and b_j is a source term for variable j .

Momentum interpolation method

For a better resolution of flow field in complex geometries, recently several investigators have developed various calculation methods of momentum equations employing the non-orthogonal, body-fitted coordinates. Among these methods, the non-staggered, momentum interpolation method originally developed by Rhie and Chow[12] is known to be one of the efficient methods and has been widely used because of its simplicity feature of algorithm. In this method, the momentum equations are solved at the cell centered locations using the Cartesian velocity components as dependent variables and the cell face velocities are obtained through the interpolation of the momentum equations for the neighboring cell centered Cartesian velocity components. In the present analysis, the modified version of the Rhie and Chow's scheme[10] is used to obtain a converged solution of unsteady flows which is independent of the size of time step.

3. Stress analysis for the piping subjected to thermal stratification

The stress analysis has performed using finite element method (FEM) for one case that the level of fluid interface is at height of 0.5di. Using ANSYS Code [7], a commercial FEM program, the stress for the thermally stratified piping has been calculated from the temperature field obtained from the above fluid analysis. Four node 2-D isoparmetric element given in ANSYS Code has been used in numerical modelling. Based on the piping symmetric condition, the half of piping cross section has been meshed with 500 elements and 561 nodes.

4. Results and discussion

The numerical solution method presented in this study was applied to the thermal stratification problem of pressurizer surge line as an example. The geometry of the surge line and most of the computational parameters used here are shown in Table 1. In operating nuclear power plants, outer surface of the pressure surge line is required to insulate. Thus, the outer surface of the surge line was assumed to be either perfectly adiabatic or diabatic with a little heat loss. Three cases of fluid interface level were investigated. The levels of fluid interface for the three cases, respectively, are at heights of $0.25 d_i$, $0.5 d_i$, and $0.75 d_i$ from the horizontal reference line passing through the bottom point of inner wall surface, where d_i is the inner diameter of the surge line.

For simplifying the calculations, on the basis of the assumptions that the fluids are Newtonian with constant properties and the Boussinesq approximation is valid, the variables of length, time, velocity and temperature are nondimensionalized, respectively, using the reference scales of r_i , $(r_i / g\boldsymbol{b}\Delta T)^{1/2}$, $(g\boldsymbol{b}\Delta T r_i)^{1/2}$, and $\Delta T = (T_h - T_c)$, where r_i is the inner radius of the surge line. For all cases, the dimensionless time step used in the computations is 0.1. The iterative computation for each

time step ceases when the maximum of the absolute sum of dimensionless residuals of momentum equations or energy equation, or pressure correction equation is less than 10^{-6}. Relaxation factors of 0.7 and 1.0 were used for momentum equations and for energy equation, respectively. The typical results of computations are transiently visualized at some selected times with a series of dimensionless stream function contours and dimensionless isotherms.

Fig. 5 is the transient stream function contours for the three cases of different fluid interface levels. As can be seen in Fig. 5, natural convection occurs more intensively in the hot fluid region than in the cold fluid region because of the high temperature difference between the hot fluid and its surrounding pipe wall and cold fluid. The mixing of the hot and cold fluids occurs very slowly as time elapses, so that it takes a lot of time till the steady-state condition is made. Little mixing is observed between the hot and cold fluids, while a more intensive mixing takes place in the edge region of the fluid interface. This is due to the conduction heat transfer within the pipe wall in the circumferential direction.

Fig. 6 displays the transient isotherms for the three cases mentioned above. In the early stage, the temperature gradient is very steep in the hot fluid region near the inner wall surface and the fluid interface, as can be expected. As time elapses, the temperature difference between the top and bottom positions of the pipe wall increases to a maximum value and then decreases to zero.

Fig. 7 shows also that the temperature gradients in the radial direction in the top and bottom regions of the piping wall are higher than in the midpoint region at the same level of fluid interface.

Fig. 8 presents the variation of the local Nusselt number as a function of the angle at 3 different elapsed times for the interface levels of $0.25d_i$, $0.5d_i$ and $0.75d_i$. The average Nusselt number decreases to zero with elapsing of time, and increases with increasing the amount of hot fluid flowing into the pipe section. These are plausible from the fact that the greater the difference in temperature between the fluid and the wall surface, the higher the Nusselt number. It is known that the major effect of thermal stratification in the pressurizer surge line of operating nuclear power plants are displacements, bending, and associated stresses resulting from a significant top to bottom temperature difference, which was not considered in the original design. In addition, axial stratification profile affects both the local stresses and the global bending effect at a given pipe cross-section. Therefore, the top to bottom temperature difference and distribution as well as their variation along the axial direction of pipe are the most important factors to be examined in the assessment of the piping integrity.

Fig. 9 displays the transient circumferential wall temperature distributions for the case of the fluid interface level, $0.25d_i$, and Fig. 10 shows the transient top to bottom wall temperature differences both at the inner and outer wall surfaces for the three different cases of fluid interface levels. As can be seen in Figs. 9 and 10, the maximum value of the temperature difference is higher at the inner wall surface than that at the outer wall surface. It increases to their maximum values at the elapsed dimensionless time zone ranging from 500 to 1500 and then decreases as time elapses further. Figs. 9 and 10 also show that the maximum top to bottom temperature difference is affected by the axial stratification profile that is characterized by the variation of fluid interface level. The piping section at which the maximum top to bottom temperature difference is produced is expected to be the case where the fluid interface level is slightly at the height of $0.5d_i$.

Figs. 11(a) and 11(b) show the non-dimensional transient temperature variations with the change in the fluid interface level at the bottom and mid-level positions on the inner and outer wall surfaces of the subjected piping at the specified non-dimensional times of 800 and 1500. As shown in the figures, the temperatures decrease as the interface level increases and the gradients of temperature distributions at the mid-level positions are steeper than at the bottom-level positions. In addition, it can be re-confirmed from those figures that the temperatures on the inner wall surface are much higher than on the outer wall surface during the early transient time period. As can be expected, such effects may cause the excessive longitudinal and circumferential stresses in the piping wall, which can eventually result in unacceptable mechanical damages to the piping such as global bending, dislocation, failure, etc.

The hoop stress σ_h and radial stress σ_r due to thermal stratification have been obtained at the cross section of piping under the fluid pressure of 2250psi using the predicted transient temperature distributions in the piping wall. The hoop stress and radial stress are normalized using the pressure hoop stress σ_{h-p} given by

$$\sigma_{h-p} = p r_i / t_w \tag{10}$$

, where p is the fluid pressure, and $t_w (= r_o - r_i)$ is the pipe wall thickness. The normalized hoop stress and normalized radial stress are defined as σ_h / σ_{h-p} and σ_r / σ_{h-p}, respectively.

Fig. 12 shows the comparison of the non-dimensional hoop stress with the non-dimensional radial stress along the pipe wall at fluid interface at the non-dimensional time of 1000. The radial stress is -2250 psi at pipe inner surface and zero at pipe outer surface. The effect of the radial stress on the pipe damage is smaller than the hoop stress because the radial stress is about 30% of hoop stress at pipe inner surface and the radial stress near pipe outer surface is negligible due to free surface effect. It means that the hoop stress may plays an important role in the evaluation of piping damage due to the thermal stratification.

The variation of the hoop stress along the pipe wall at fluid interface at the non-dimensional times 0, 1000, and 2500 is shown in Fig.13. The hoop stress near pipe inner surface decreases up to the non-dimensional time 1000, and increases again. If there is no fluid pressure in piping, the compressive hoop stress would be applied at the piping inner surface.

Fig. 14 shows the hoop stress as a function of time at such locations as pipe inner surface r_i, 10% wall thickness from the pipe inner surface r_c, middle of the pipe wall r_m, and pipe outer surface r_o. As shown in the figure, the hoop stresses at r_i and r_c decrease rapidly and increase again as the time increases. It means that the fatigue damage due to thermal stratification is very large near the pipe inner surface. If there is a crack near the pipe inner surface, the crack would grow due to the fatigue damage. The further study on the crack behavior near the pipe inner surface is required.

5. Conclusions

An efficient numerical method for calculating the thermally stratified flows in horizontal circular pipes has been presented. The method employs a body-fitted non-orthogonal grid system to accommodate the pipe wall of circular geometry and the interface of two fluids at different temperatures of which the level is variable, in the calculations.

The transient behaviors of fluid flow and temperature distribution in the piping were simulated using the finite volume approach. The convection term is approximated by a higher-order bounded scheme named COPLA, which is known to be a high-resolution and bounded discretization scheme. The cell-centered, non-staggered grid arrangement is adopted and the resulting checkerboard pressure oscillation is prevented by the application of modified momentum interpolation scheme. The SIMPLE algorithm is employed for the pressure and velocity coupling.

The method proposed in this study was applied to the thermal stratification issue of pressurizer surge line, and the results have been discussed in detail. The results showed that the present method is applicable for the solution of thermal stratification problem.

In addition, numerical stress analyses for the thermally stratified piping have been performed using the predicted transient temperature distributions in the piping wall exposed to internally stratified flow. Non-dimensional hoop stress and radial stress as a function of time have been obtained along the piping wall. The result shows that thehoop stress near the pipe inner surface decreases rapidly and increases again as the time increases. It means the fatigue damage due to thermal stratification is very large near the pipe inner surface.

Although this paper addressed only one special case, it is emphasized that the present method can be extended for applications to various cases of thermally stratified flows in pipes and tanks with complex geometry and different flow conditions.

References

[1] NRC (1988), "Thermal Stress in Piping Connected to Reactor Coolant System," NRC Bulletin No. 88-08.

[2] NRC (1988), "Pressurizer Surge Line Thermal Stratification," NRC Bulletin No. 88-11.

[3] Smith, W.R., et al. (1988), "A solution for the Temperature Distribution in a Pipe Wall Subjected to Internally Stratified Flow," Proceedings of the 1988 Joint ASME-ANS Nuclear Power Conf., Myrtle Beach, South Carolina, pp. 45-50.

[4] Talja, A., and Hansjosten, E. (1990), "Results of Thermal Stratification Tests in a Horizontal Pipe Line at the HDR-Facility," Nucl. Eng. and Design, Vol. 118, pp.29-41.

[5] Ensel, C., et al. (1995), "Stress Analysis of a 900 MW Pressurizer Surge Line Including Stratification Effects," Nucl. Eng. and Design 153, 197-203.

[6] Yu, Y.J., et al. (1997), "Structural Evaluation of Thermal Stratification for PWR Surge Line," Nucl. Eng. and Design 178, 211-220.

[7] ANSYS Code (1996), Ver.4.4, Swanson Analysis Systems Inc.

[8] Jung, I.S., et al. (1996), "Thermal Stratification in a Horizontal Pipe of Pressurizer Surge Line,"Transactions of KSME; B, Vol.20, No.4, 1449-1457.

[9] Choi, S. K., Nam, H. Y. and Cho, M. (1995), "Evaluation of a Higher-Order Bounded Scheme: Three-Dimensional Numerical Experiments," Numerical Heat Transfer, Part B, Vol. 28, pp. 23-28.

[10] Jo, J. C., Kim, Y. I. and Choi, S. K., "Heat Transfer Analysis of Thermal Stratification in Piping Connected to Reactor Coolant System.": in Proc. of the 1st Korea-Japan Symposium on Nuclear Thermal Hydraulics and Safety, Paper No. WR-13, pp.191-198, 1999.

[11] Patankar, S. V., Numerical Heat Transfer and Fluid Flow, McGraw-Hill, New York, 1980.

[12] Rhie, C. M., and Chow, W. L. (1983), "Numerical Study of the Turbulent Flow Past an Airfoil with Trailing Edge Separation," AIAA J., Vol. 21, No. 11, pp. 1525-1532.

Table 1. Computational parameters

Parameters	**Values**
Material of pipe	SA-762-TP-316
Outer radius of pipe, r_o	0.1525m
Inner radius of pipe, r_i	0.1165m
Conductivity of pipe, k_s	15.4 W/m°C
Heat transfer coef., h	15.4 W/m^2°C
Hot fluid temp., T_h	232 °C
Cold fluid temp., T_c	66 °C
Ambient temp., T_∞	43 °C
Thermal diffusivity ratio, a_s/a_f	22.2
Thermal conductivity ratio, k_s/k_f	22.65
$Gr\left(=\frac{g b_f r_f^2 r_i^3 (T_h - T_c)}{m_f^2}\right)$	1.938×10^{10}
$Pr\left(=\frac{c_{pf} m_f}{k_f}\right)$	1.1712
$Bi\left(=\frac{h(r_o - r_i)}{k_s}\right)$	1.87×10^{-3}

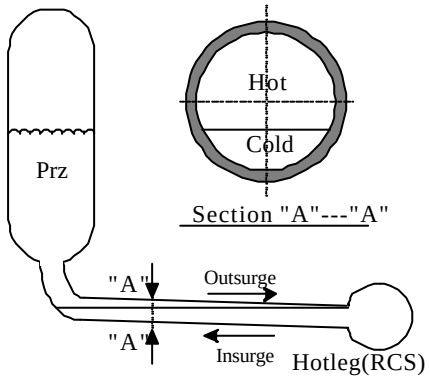

Fig. 1 Thermally stratified flow ina circular piping.

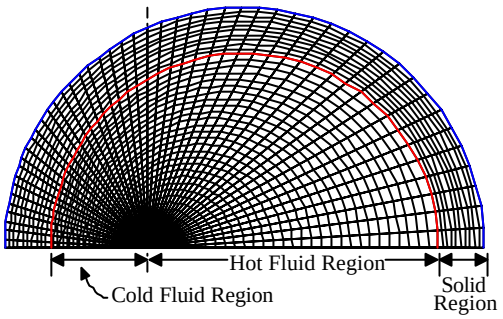

Fig. 2 The curvilinear non-orthogonal mesh.

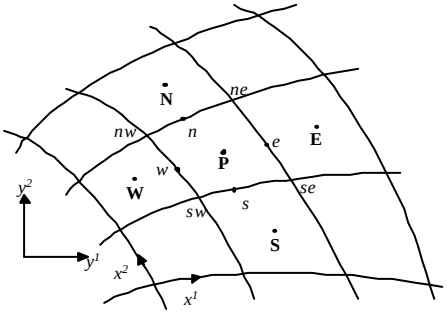

Fig.3 Typical control volume cell in the computing mesh.

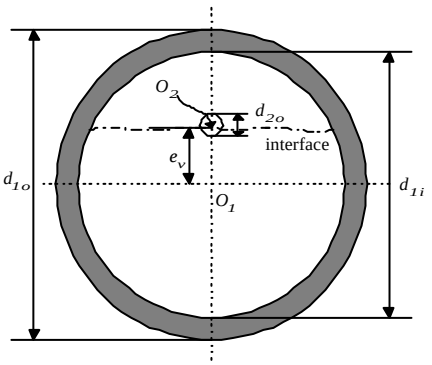

Fig.4 The imaginary cylinder model for mesh generation.

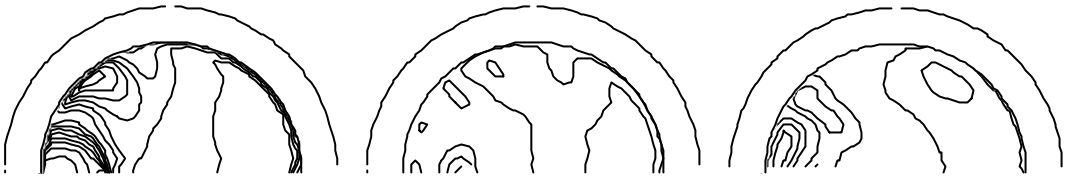

a) Lvl 0.25d_i, time = 100[-3E-5 (3E-6) 2E-5], 1000[-9E-6 (3E-6) 9E-6], 1500[-4E-6 (1E-6) 2.5E-6]

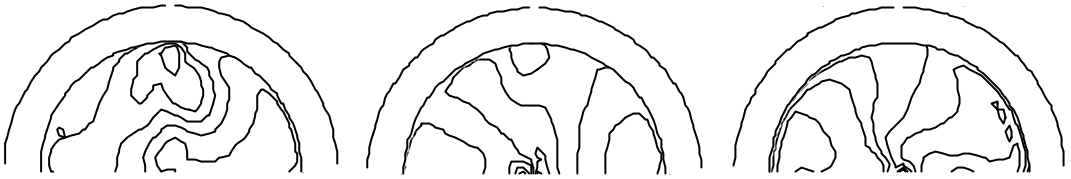

b) Lvl 0.5d_i, time = 100[-7E-6 (3E-6) 1E-5], 1000[-1E-5 (3E-6) 9E-6], 2000[-1E-5 (3E-6) 9E-6]

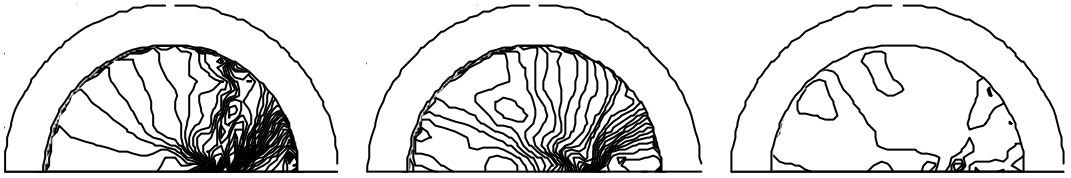

c) Lvl 0.75d_i, time = 100[-8E-5 (3E-6) 6E-6], 1000[-3E-5 (2E-6) 3E-5], 2000[-1.3E-5 (3E-6) 6E-6]

Fig. 5 Transient stream function contours in case where the outer surface of pipe is perfectly insulated

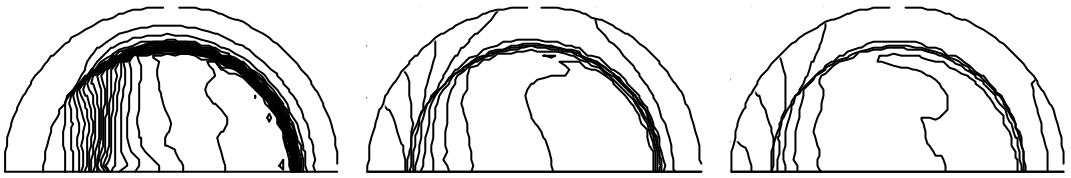

a) Lvl 0.25d_i, time = 100[0.05(0.05)1.0], 1000[0.15(0.05)0.6], 1500[0.25(0.05)0.55]

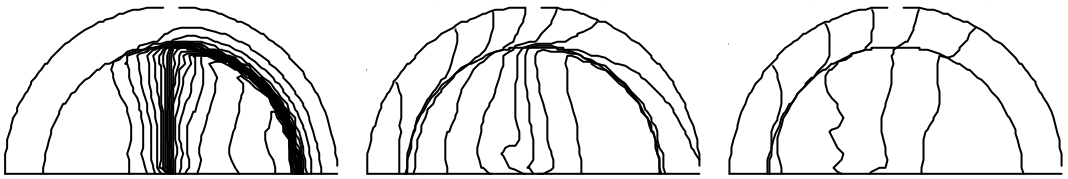

b) Lvl 0.5d_i, time = 100[[0.05(0.05)0.95], 1000[0.05(0.05)0.45], 2000[0.05(0.05)0.40]

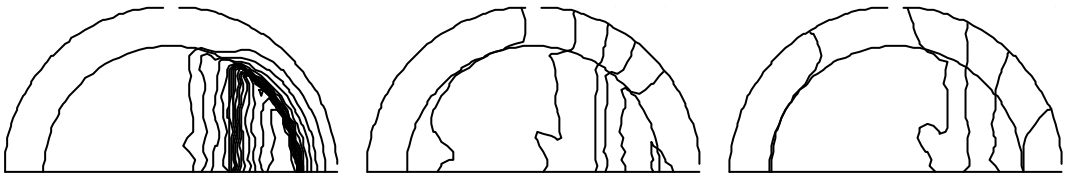

c) Lvl 0.75d_i, time = 100[0.05(0.05)0.8], 1000[0.05(0.05)0.3], 2000[0.05(0.05)0.3]

Fig. 6 Transient isotherms in case where the outer surface of pipe is perfectly insulated.

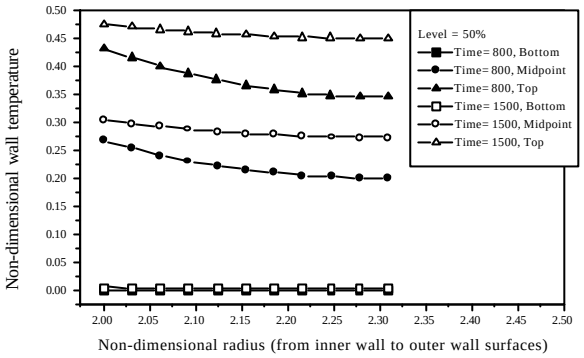

Fig. 7 Temperature gradient in the radial direction at the top and bottom levels.

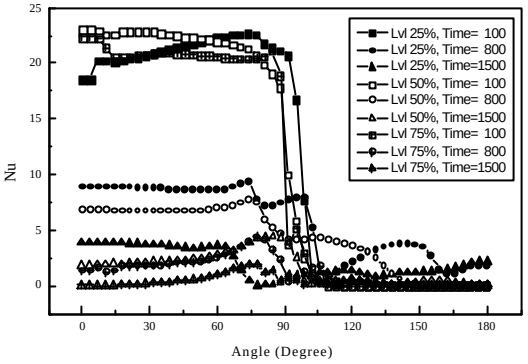

Fig. 8 The variation of the local Nusselt number(Nu).

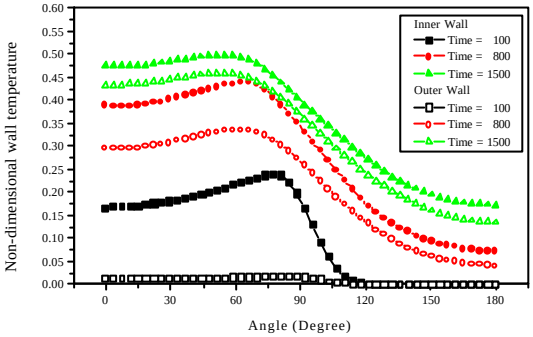

Fig. 9 Top to bottom wall temperature distributions for the level $0.25d_i$.

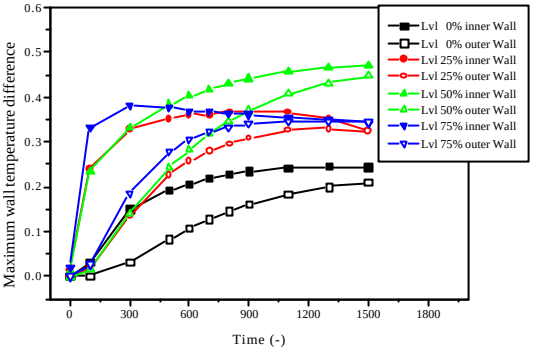

Fig. 10 Maximum wall temperature differences both on the inner and outer wall surfaces.

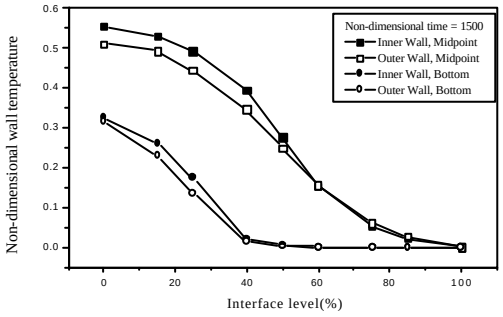

(a) Non-dimensional time = 800.

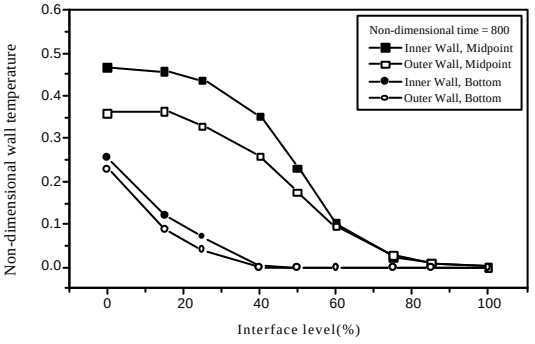

(b) Non-dimensional time = 1500.

Fig. 11 Non-dimensional temperatures on the inner and outer wall surfaces at the bottom and mid-level positions.

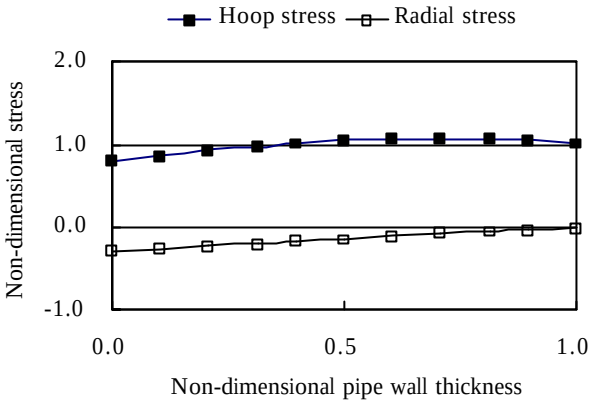

Fig. 12 Comparison of non-dimensional hoop stress with non-dimensional radial stress along the pipe wall at fluid interface at the non-dimensional time=1000.

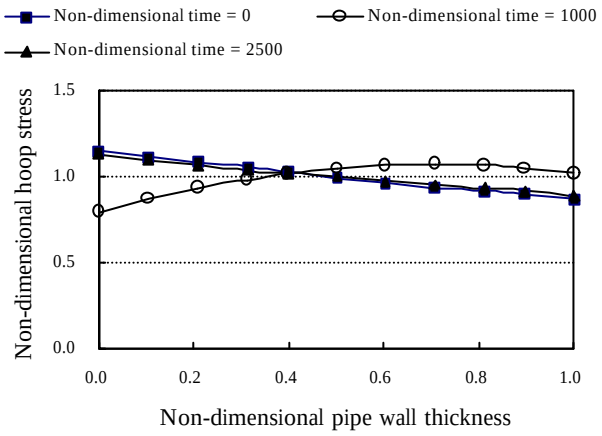

Fig. 13 Variation of hoop stress along the pipe wall at fluid interface at the non-dimensional times =0, 1000, and 2500.

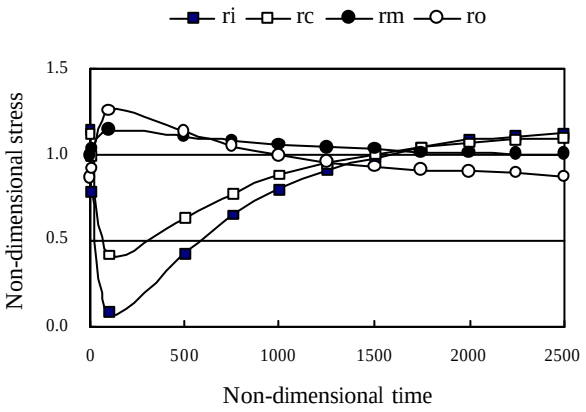

Fig. 14 Hoop stress as a function of time at pipe inner surface(r_i), 10% wall thickness from the pipe inner surface(r_c), middle of the pipe wall(r_m), and pipe outer surface(r_o).